PROCEEDINGS OF SCIENCE

GRB 210905A at $z = 6.3$: a powerful blast from the past.

PoS(MULTIF2023)070

Massimiliano De Pasquale[a,b,*]

[a] *MIFT Department, University of Messina, Viale F.S. D'Alcontres 31, 98166 Messina, Italy.*

[b] *This work mostly summarizes the analysis and the results of the article by Rossi, A. et al. 2022 (see references).*

E-mail: masdepasquale@unime.it

I shall be discussing the Gamma-ray Burst 210905A, an event *both* extremely powerful - with a energy release of $\simeq 10^{54}$ erg - and extremely remote, being at redshift 6.3. The afterglow of this burst appears to be the most luminous of all Swift GRB afterglows at $\simeq$ 1 week after the trigger. This GRB grabs the attention also because its prompt emission might be unusually attributed to forward shock emission, while the afterglow appears to go through energy injection for almost one day. A jet break seems to be present as well, but it occurs late, indicating that high-z bursts may not have narrower jets that closer GRBs. I also discuss briefly the spectroscopic observations of this remote but extremely luminous "beacon" that have brought around a trove of data about the abundance of metals and their status in the host galaxy, when the Universe was less than one billion years old. Despite being very bright and distant, GRB 210905A seems just to be in the "high energy tail" of long GRBs, without properties that may let us think that its progenitor was unusual, for example a Population III star.

Multifrequency Behaviour of High Energy Cosmic Sources XIV (MULTIF2023)
12-17 June 2023
Palermo, Italy

*Speaker

1. Introduction

Gamma-ray Bursts (GRBs) are the most luminous explosions in the Universe, reaching luminosities $L \sim 10^{52} - 10^{53} s^{-1}$ for a few hundreds seconds [1]. They are associated to either the explosion of a massive star (long or Type II GRBs, [2]) or the merger of two compact objects, such as two neutron stars (short or Type I GRBs, [3]). GRBs are cosmological sources, found from very low to very high z. They are an excellent laboratory for extreme Physics, and at the same time very luminous "beacons" to shed light on the environment at very high redshift[4]. There is no selection for galaxy size; only star formation is needed (at first order) to produce GRBs. Nonetheless, it is not always easy to study bursts since they are fading transients, and GRBs at very high redshift are discovered rarely ($0.5 - 1$ bursts at $z > 5$ / year). Among the missions principally directed to study GRBs, there is the Swift Neil Gehrels Observatory (Swift, [5]), with its Burst Alert Telescope (BAT; 15-350 keV; [6]), the X-ray Telescope (XRT; 0.3-10 keV; [7]) and the UV/Optical Telescope (UVOT; 170-650 nm) ; [8]). Another mission to study GRBs is the Konus-Wind spacecraft [9, 10], which carries sensors operating in a 20-1500 keV energy band and providing omni-directional sensitivity to GRBs. Swift detects 90 GRBs / year with BAT and slews autonomously to observe the burst with its XRT and UVOT from $\sim$ 100 s after the burst trigger.

Swift BAT triggered on the exceptional GRB 210905A [11] while KW observed it in the so called "waiting mode" between 20 and 1500 keV [12]. This GRB proved to be a rare example of very bright GRB at high redshift and showed what luminous GRB can do for us to explore the ancient Universe.

2. Event Description

GRB 210905A is a long burst, with $T_{90} \simeq 870$ s, where T_{90} is the time interval in which the instrument collected 90% of the counts coming from a transient source. Only Konus-Wind (KW), orbiting distant from Earth, was able to catch the entirety of the prompt, high-energy emission. This is composed of 3 main episodes (see Fig.1).

The Swift XRT and the UVOT started observations at trigger time $T_0 + 92$ s and $T_0 + 156$ s respectively; other than observing, Swift was disseminating to other observatories the coordinates of the new burst. Thus, the Rapid Eye Mount (REM) near infrared robotic telescope [13] could start observations about 400 s after the trigger time. The light-curves produced by the different instruments are shown in Fig.1.

While REM saw a bright source in the near infrared (NIR) bands such as H, simultaneous UVOT observations detected nothing. This is a tell-tale signature of a very high-redshift GRBs, since the Lyman-α absorption by intergalactic hydrogen is redshifted to the optical band if the source is at redshift $z > 5$ [14]. In this circumstance, the source is visible in the NIR but not in the optical. Indeed, about $\simeq 2.5$ hours after the trigger, the X-Shooter spectrograph attached to the 8.2-m VLT Unit 3 took a spectrum whose numerous features proved a redshift $z = 6.312$ [15]. Knowing the fluence thanks to KW data, which have a wide band, and the distance, it was possible to determine the energy output in the γ-ray band. Assuming isotropy, GRB 210905A emitted $E_{\gamma,iso} = 1.27 \times 10^{54}$ erg. Thus, GRB 210905 showed to be a very energetic event and to have happened at very high redshift, simultaneously. This is a rare occurrence in GRB observations,

PoS(MULTIF2023)070

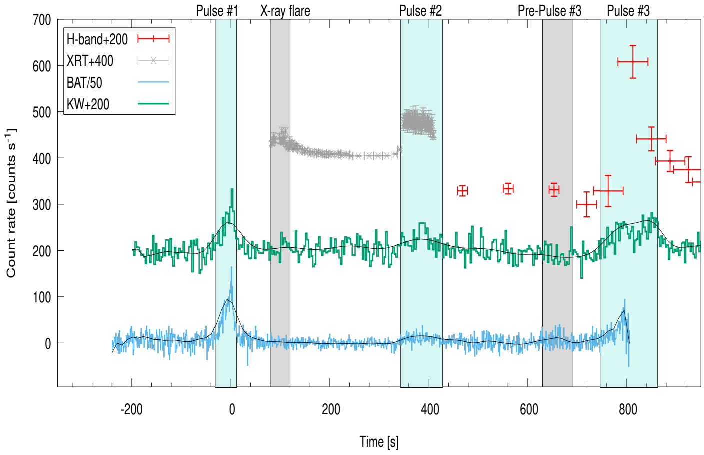

Figure 1: The high-energy, X-ray, and NIR light-curve of the prompt emission of GRB 210905A. From [16].

although we note that the farthest bursts are expected to be often the most energetic ones, due to selection effect.

3. Prompt emission

The mechanism that produces the prompt high-energy emission in GRBs is still not established, although many hypothesis have been formulated [1]. Here, we propose that the Forward Shock (FS) could be responsible for it [17]. This model explains the radiation as synchrotron emission from electrons of the medium; these are heated by a forward-moving, ultra-relativistic shock-wave created by the explosion ejecta. Hallmark of FS radiation is that the flux density depends on time and frequency as power-law: $F_\nu \propto t^{-\alpha}\nu^{-\beta}$.

Now, at low-energy, the prompt spectrum was thought in the past to be a simple power law. But [18] systematically found a low-energy break between 2 and 30 keV (sometimes up to a few 100 keV) in Swift and Fermi ([19]) GRBs. The power law "breaks" into 2, having energy indexes +1/3 and -1/2. These are consistent with FS model predicted values in the so-called "fast-cooling" case, in which the synchrotron injection frequency is larger than the cooling frequency $\nu_m > \nu_c$. Thus, we jointly fitted a double broken power-law model with the FS indexes to the data of 210905A prompt emission pulses, the X-ray flare and the pre-3rd pulse data (Fig. 2; only during the peaks/flares and the pre-3rd pulse data we have a large number of counts, as it emerges from Fig. 1, and spectral analysis can be sensibly performed). The fits of all the spectral energy distributions (SEDs) were always good. Optical data were added as well to the fit of the pre-3rd pulse and 3rd pulse as well, but the H-band datum alone won't tell if the energy index is +1/3, as predicted by synchrotron emission at low energies. Moreover, the temporal evolution of the break frequencies over the entire duration of the prompt emission is not that expected in the FS model. Perhaps each single flare/pulse is a distinct episode of FS emission, caused by a separate interaction of the relativistic

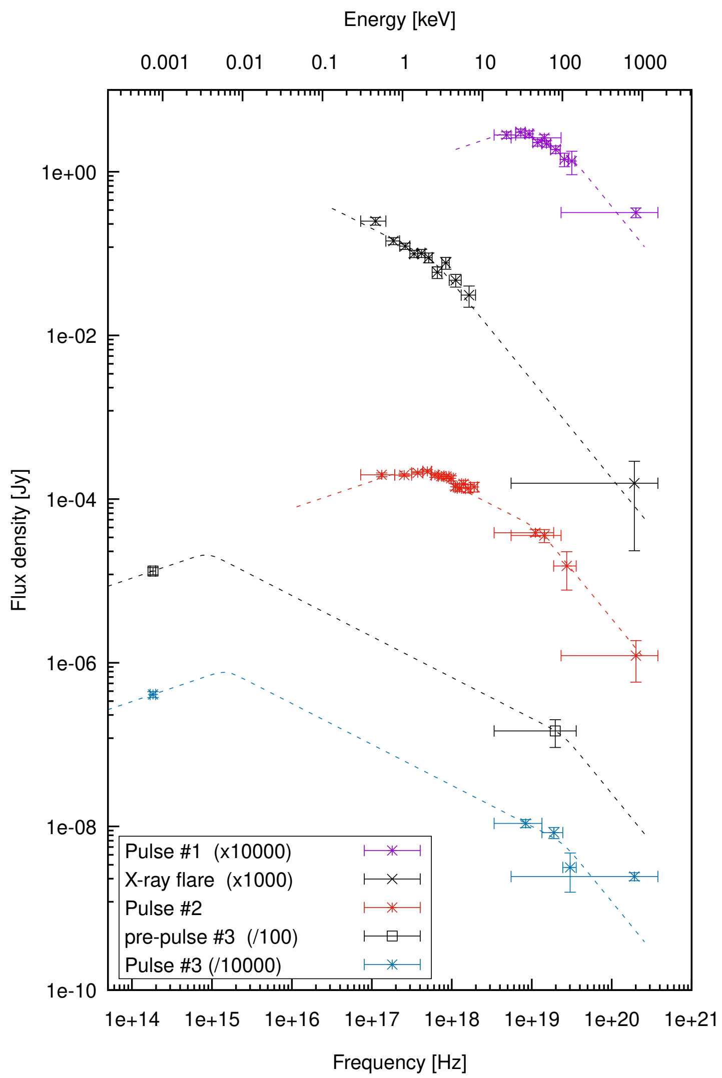

Figure 2: The high-energy, X-ray, and NIR light-curve of the prompt emission of GRB 210905A. From [16].

ejecta. Nevertheless, the prompt emission spectrum appears consistent with synchrotron. See [20] for more on this interpretation.

4. Afterglow

Following the prompt emission, a long-duration so-called afterglow emission takes place. By studying and normalizing the emission from VLT, LCO, REM, CTIO, BlancoDECam, GROND, Swift XRT (see [16] for logs and methods of data reduction), we could build up the NIR and the X-ray light-curves. The former shows an early decay index of $\alpha_{1,opt} = 0.69 \pm 0.04$, followed by a break at $t_{break,opt} = 85.9 \pm 62.7$ ks, and a late $\alpha_{2,opt} = 0.94 \pm 0.04$. While the break is loosely constrained, the improvement in $\chi^2/d.o.f.$ (degrees of freedom) is significant: from 1.36 to 0.92. The X-ray

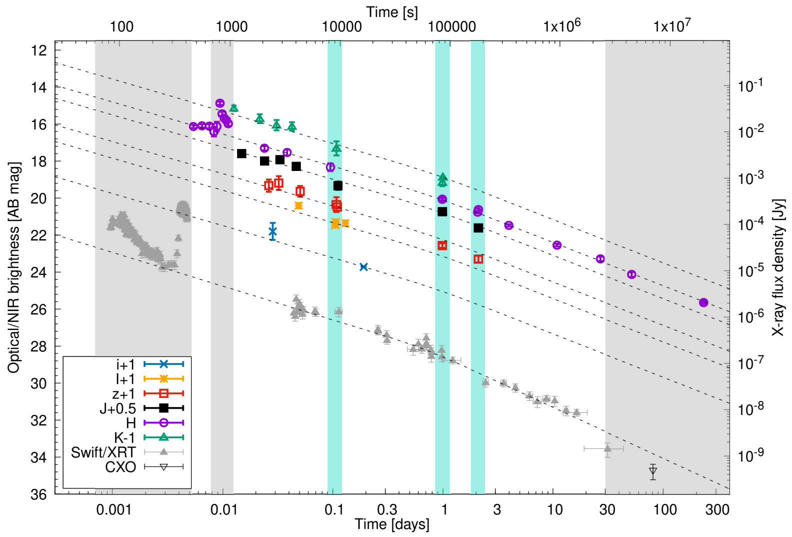

Figure 3: The NIR and X-ray light-curves. Note the presence of the break at ≃ 60ks. From [16].

light-curve, after some very early flaring, shows first a decay with slope $\alpha_{1,X} = 0.74^{+0.03}_{-0.01}$, a break at $t_{break,X} = 60 \pm 30$ ks, followed by a late decay with index $\alpha_{2,X} = 1.10 \pm 0.04$. If we fit a broken power-law model to the X-ray and the NIR data together, the break is found at $t_{break} = 60.5 \pm 22.5$ ks (Fig. 3).

We built spectral energy distributions (SEDs) at epochs 0.1, 1 and 2.2 days after the trigger time T_0, and we fitted a simple power-law and a broken power-law model to them (see Fig.4). A broken power law spectrum with $\Delta\beta = 0.5$ is expected if ν_c is between the X-rays and optical frequencies. It is not immediate to choose between the single and broken power-law model as they are fitted by the SEDs comparably well in both cases. However, at the first epoch the two models yield the same value for the low-energy spectral index: thus we conclude that ν_c is at or above the X-ray frequency. The best-fit spectral index below ν_c is found to be $\beta = 0.63$. The simple power-law model fitted to the 1 d SED yields a $\chi^2 = 75.8$ with 54 degrees of freedom, while the broken power-law model gives $\chi^2 = 63.51$ with 53 degrees of freedom. The former model is strongly favoured, since the probability of a improvement by chance is less than 0.002, calculated with the F-Test. We find $\beta_{opt} = 0.60 \pm 0.04$ and a break in the low X-energy region. As in the case of the first SED, the simple power-law and the broken power-law models can be fitted both equally well to the last SED, but data are not of very good quality. Thus, to fully understand the picture, one needs to consider the light-curves. Let us examine the 1 d SED. If we assume that the break is ν_c, then $\beta_X = \beta_{opt} + 0.5 = 1.10 \pm 0.04$. The FS predicts $\alpha_X = 1/2(3\beta_X - 1) \simeq 1.15$ for $\nu_X > \nu_c$, which is consistent with the observed $\alpha_{2,X} = 1.10 \pm 0.04$. The optical band is still below ν_c; in this case, $\alpha_{opt} = 3/2\beta_{opt} \simeq 0.9$, which is again consistent with observations. In the last SED, 2.2 days after the trigger, the spectral index in the X-ray and in the optical band have not significantly changed, so the decay slopes do not change with respect those at 1 day, as we actually see. As for the early decay at 0.1 d, the decay slopes of the optical and the X-ray flux are consistent, and this is again in agreement with the FS model, in which ν_c moves redwards as time goes by. Thus, ν_c was at an

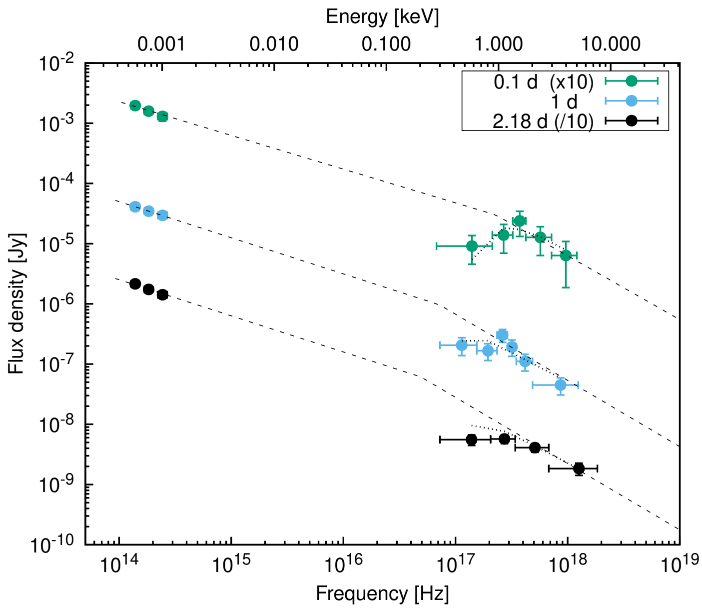

Figure 4: NIR - X-ray spectral energy distributions at 0.1, 1 and 2.2 days after the trigger. From [16].

energy larger than the X-ray band at such an early epoch. Therefore, the X-ray and optical have the same decay slope because they are on the same spectral segment of the FS spectrum, between ν_m and ν_c. However, the decay slope before the $\simeq$ 60 ks break is too shallow to be interpreted as simple FS emission. We attribute such a shallow slope to mild energy injection into the ejecta, which finishes at $\simeq$ 60 ks. Such a termination causes the flux to decay faster at all wavelengths, as we note. If the energy injection [21] is powered by late shells that merge with the trailing ones, one can demonstrate that if the mass M of the trailing shells goes as $M(>\gamma) \propto \gamma^{-1.45}$, where γ is their Lorentz factor, then the decay slopes before the break are reproduced.

The afterglow of GRB 210905A, both in the X-ray and optical band, is one of the most luminous, *if not the most luminous one ever registered by the Swift mission.* This can be seen in Figure 5. At an epoch $t = T_0 + \simeq 1$ week, GRB 210905A is more luminous than all afterglows seen by Swift. One may thus wonder if this burst is a “normal" long GRBs or has some other properties that differentiate it from the bulk of Swift GRB. However, this does not appear to be the case: in figure 6, one can see that the Amati relation [22], followed by long GRBs, is fully satisfied by the burst as a whole and even by single pulses; the Yonetoku [23] and the Ghirlanda [24] (in which the energy is corrected for beaming factor; see later) relations are satisfied by this event as well. A key observation is the ratio between the energy emitted in γ-rays and the afterglow X-ray luminosity: as we can see from Fig. 7, this ratio is *en par* with less energetic events [25]. Thus, we argue that GRB 210905 just belongs to the high-energy tail of long GRBs. It does not exhibit other properties that might make us believe that it has a different kind of progenitor, for example a Population III star.

The Chandra X-ray observatory performed an observation about 81 days after the trigger [26], and the flux was below the extrapolation of XRT ligh-curve. Thus, a break to a steeper decay seems to be required. Late-time steepening in a GRB light-curve is usually a jet break [27]. The

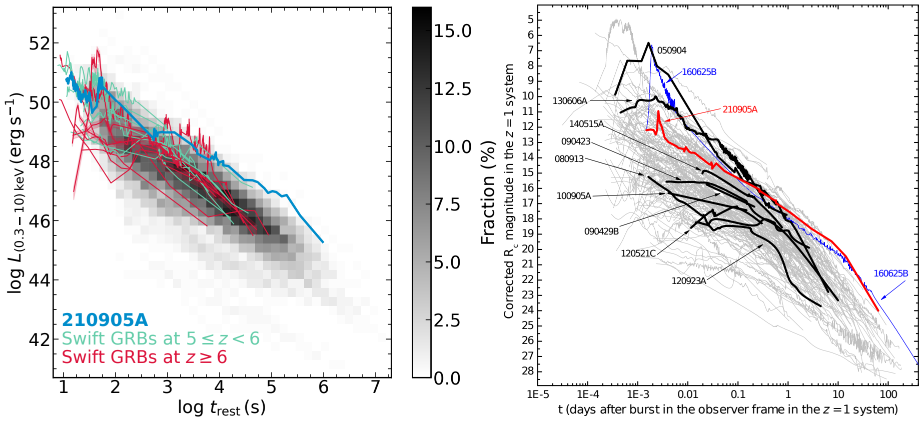

Figure 5: X-ray (left) and Optical-NIR (right) light-curves of GRB 210905A against the GRB light-curves up to 2020. From [16].

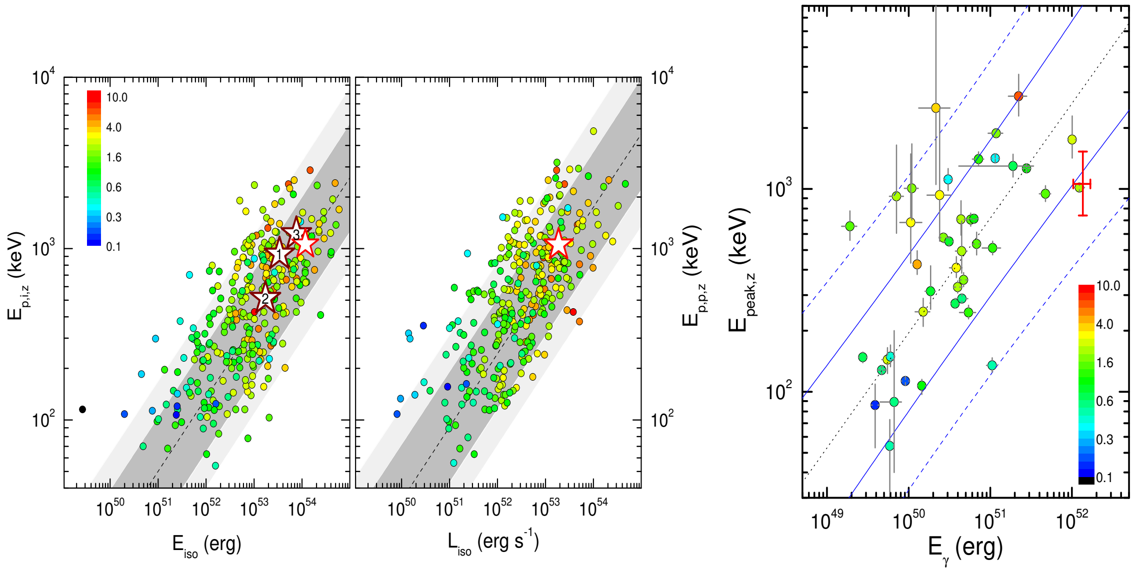

Figure 6: Prompt emission and relations. Left: GRB 210905 in the Amati (prompt E$_{\gamma,peak}$ vs E$_{\gamma,iso}$) relation. Even single pulses of the prompt emission satisfies the relaiton. Centre: the Yonetoku relation (L$_{iso}$ vs E_{peak}). Right: Ghirlanda (prompt E$_{\gamma,peak}$ vs E$_{\gamma,beam}$) relation. GRB 210905A is the red cross. From [16].

emitting, expanding source is not isotropic, but it is jet-like. The ejecta decelerate by piling up circumburst medium, and the beaming angle of the radiation gets wider and wider; thus more and more emitting surface is visible by the observer. At a certain epoch, the Lorentz factor Γ will be such that $\Gamma^{-1} \simeq \theta_{jet}$, where θ_{jet} is the opening angle of the outflow and Γ^{-1} is the rough beaming factor. At this time, the observer sees the emission coming from all the emitting surface. At this time, the flux light-curve will show a break to a quite steeper decay, $\alpha \simeq p$. Since, in the FS model, the spectral index $\beta(\nu_{obs} < \nu_c) = \frac{p-1}{2} \simeq 0.6 \implies p \simeq 2.2$, we can infer that the post jet break

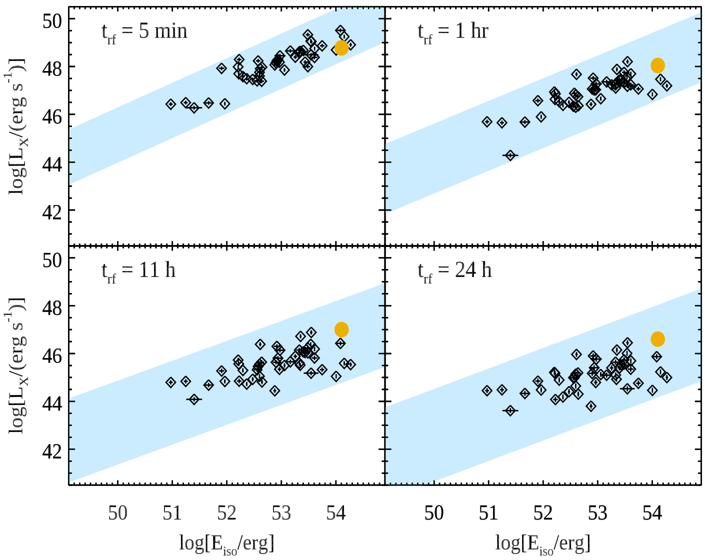

Figure 7: The relation between the isotropic value of energy emitted during the prompt phase and the afterglow X-ray flux at different epochs. GRB 210905 (yellow dot) has a ratio similar to that of other GRBs (black dots). From [16].

decay slope will be $\alpha_{jet} \simeq 2.2$ [27]. Such a decay slope must be present in the optical band as well as in the X-ray band.

We fitted a broken smooth power-law (some jet breaks shows a smooth steepening; this could be due to the crude model approximation that does not capture details, such as a slight off-axis view) model the X-ray light-curve from the early break till the Chandra data point with the late steep slope fixed to 2.2. In the X-ray, the fit is statistically acceptable and yields a break time $t_{jet} = 46 \pm 16$ days. However, the H-band light-curve shows an opposite behaviour: it flattens at very late epochs (see Fig. 8). We took HST imaging of the GRB 230 days after the trigger (to avoid any residual afterglow contamination), and we found that at the position of the GRB afterglow, a H-band source is present, possibly the host galaxy of the burst. We found that this source has magnitude $H = 25.8 \pm 0.2$. This corresponds to a rest-frame magnitude $m_{1900} \approx -21$, typical of star-forming galaxies at $z = 6 - 7$ [16, 28]. Such an object is likely responsible of the H-band light-curve flattening. The FS model predicts a relation between the isotropic kinetic energy of the ejecta, the density of the circumburst medium, and the opening angle of the jet[29]: $\theta_{jet} = 0.12(\frac{E_{kin,iso,53}}{n})^{-1/8}(\frac{t_{jet,d}}{(1+z)})^{3/8}$ rad. We have the value of energy emitted isotropically in γ-rays; to calculate the kinetic energy we assume an efficiency in converting the total energy into γ-rays $\eta = \frac{E_\gamma}{E_\gamma + E_K} \simeq 0.2$ [30]. Under such assumption, and taking $n = 1$ cm^{-3}, we find $\theta_{jet} \simeq 0.15$ rad. Knowing the opening angle, we can compute the true, beaming-corrected energy emitted in γ-ray and the total (kinetic + γ-ray): $E_{\gamma,beam} \simeq 1.4 \times 10^{52}$ and $E_{tot,beam} \simeq 7.2 \times 10^{52}$ erg. The opening angle of the jet appears to be larger than that of other events at very high redshift, thus suggesting that it not true that these events have narrower jets than GRBs at lower z, as suggested by a few authors (see [16] and references therein). The opening angle of the jet is a critical parameter, because it enables us to constrain the star formation rate at very high redshift. Wider jets implies that we are missing less of them, thus the star formation

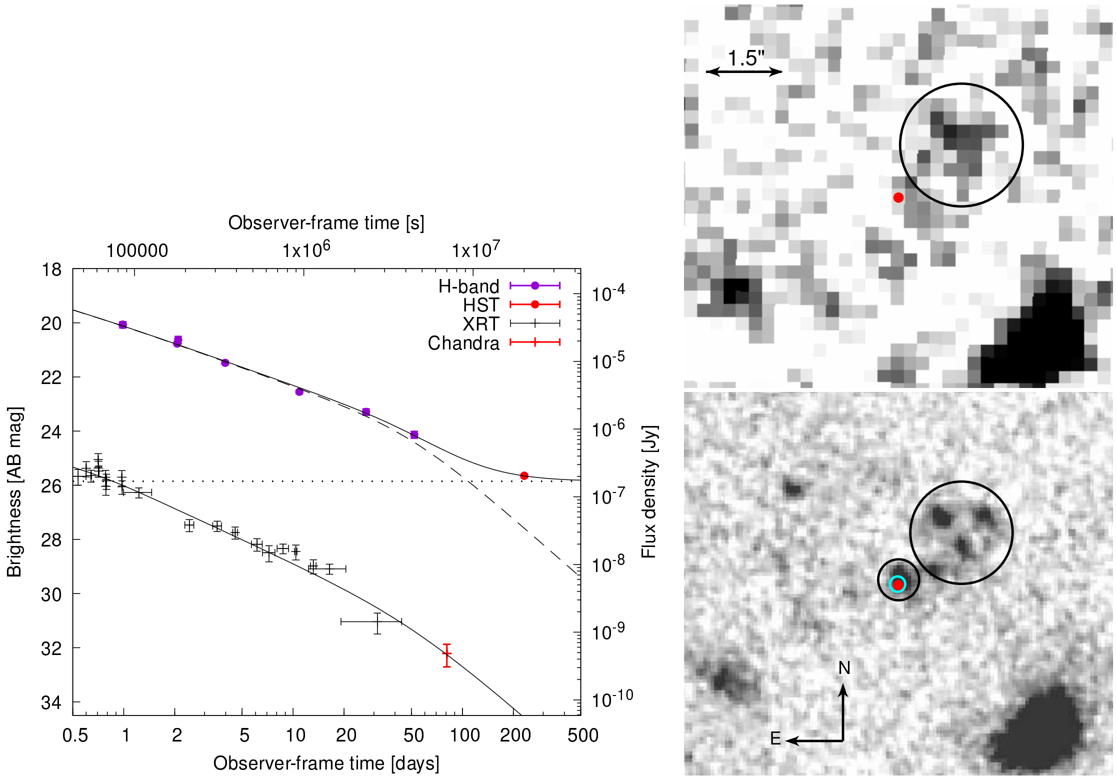

Figure 8: Left: the late X-ray and NIR light-curves of GRB 210905. Right left: VLT imaging of the afterglow region. Right bottom: HST imaging. The afterglow (red dot) is basically located on its host galaxy. Thus, the late optical light-curve flattens, without showing any jet break steepening. The blue circle is the Chandra error region. Other objects appear close to the host. From [16].

rate at that redshift cannot be too high (note that these estimates do not require to detect the host galaxies). We note, however, that the hypothesis that GRBs at very high redshift have narrower jets is not excluded by this single finding of a very energetic burst with a broad jet.

Determining the energy "budget" of the burst is important because it can inform us on its so-called "central engine". At present, two candidates for central engine of long GRBs are considered by the community. The first is a newly born and massive magnetar ([31, 32]) with an initial millisecond period and magnetic field of $\sim 10^{15}$ Gauss, producing dipole radiation, and the second is a Kerr black hole of a few solar masses just produced in a "failed" supernova (in the sense that the shock wave from the stellar core fails to blow away most of the star mass, and inner regions of the stellar body collapse into a black hole [2]) and surrounded by an accretion disk. From the black hole - disk system, the Blandford-Znajeck[33] mechanism extracts energy and funnels plasma into two jets. Such central engines can be also responsible for the large luminosity of supernovae associated to GRBs. The magnetar appears to be an unlikely engine for GRB 210905A: in fact it can release up to a few 10^{52} erg, 10^{53} erg in the most optimistic cases. But even so a too high efficiency in the conversion of dipole radiation into energy emitted into the burst would be required. On the other hand, even a $\sim 10\ M_{\odot}$ black hole has got a few $\sim 10^{54}$ erg of rotational kinetic energy that can be extracted. Observations over the last decades have shown that black holes of such masses do exist.

5. The NIR spectrum of GRB 210905A: a profusion of information about a remote and ancient star forming galaxy.

The X-shooter NIR spectrum of luminous GRB 210905A shows a plethora of features, which are attributed to the medium of the host galaxy. Since this event occurred at $z = 6.3$ and in a star forming galaxy (long GRBs are associated to star forming galaxies), we have the exciting chance of examining the medium of a star forming galaxy when the universe was less than 1 billion years old. Of course we are going to study only the material along the "pencil beam" of GRB radiation, but the medium of a $H = 26$ mag galaxy could not be studied globally even with a 8-m class telescope. The study of the afterglow NIR spectrum is presented in great details in [28]. Here, we give a summary (see Fig. 9). Two systems are present in the host spectrum, showing a relative velocity of 360 km/s. The systems show low ionization lines, namely C II, O I, Mg II, Al II, Si II, S II, Fe II, and high ionization lines, namely C IV, N V, Si IV. Even fine lines, caused by the UV pumping (i.e. excitation) of the GRB radiation, are present: C II*, Si II*. The abundances of such species indicates that they were produced in ”normal" core collapse SNe and massive Asymptotic Giant Branch stars. There is no evidence of anomalous abundances we could put down to very massive Population III stars, as already mentioned. If we use the amount of Silicon and the amount of atomic Hydrogen derived from the NIR spectrum (the host galaxy spectrum is basically a Damped Ly-α object, DLA, for which we find $\log NH_I = 21.1 \pm 0.1$ cm^{-2}), we can derive a metallicity of the host galaxy which is $\log[M/H]_{tot} = -1.71 \pm 0.12$. We used Silicon since Iron is subject to coalesce into dust grains. Remarkably, this is the same result obtained by considering all the element features seen in the spectrum and correcting for α-elements enhancement: $\log[M/H]_{tot} = -1.72 \pm 0.13$ Significant dust depletion is present: considering the elements Zn and Fe, the former hardly subject to dust condensation and the latter strongly prone to it, we find $[Zn/Fe] = 0.33 \pm 0.09$. The dust-to-mass (DTM) ratio, that is the ratio between the mass of dust and the global mass of the metals present, is DTM $= 0.18 \pm 0.03$; it means that $\simeq$ 18% of metals of this galaxy, at that time and stage of evolution, are locked in dust. Metallicity and DTM are similar to that of other objects, such as QSO-DLA and other GRBs, found at high redshift.

6. The need for missions to study very high-redshift GRBs

Very high redshift bursts ($z \gtrsim 6$) such as GRB 210905A attract a great interest in the GRB community, because they can be used as very powerful “beacons" to explore the ancient Universe: the early galaxies - even those invisible to HST and JWST -, star formation, metal enrichment in the primordial Universe, and the process of reionization. However, Swift detects only $\sim 0.5 - 1$ yr^{-1} event at $z > 5$. A much larger number of events at very high redshift is believed to occur ([34]; Aksulu et al., priv. comm.), but we are not currently equipped to detect them. It has been calculated that, in order to achieve the aforementioned scientific goals, we need the detection and follow-up of a few tens of GRBs at $z > 6$ [35], and in turn this is possible only with trigger instruments $\sim$ 10 times as sensitive as those on Swift and that keep such a sensitivity down to $\sim$ 0.5 keV, and have a large field-of-view. The proposed Transient High Energy Sky and Early Universe Surveyor (THESEUS; [35]; see Fig. 10) aims at achieving the above targets. It is planned to carry 3 instruments: the soft X-ray imager (SXI, 0.3-6 keV) lobster-eye telescope, convering $\simeq$ 0.5 sr at any given time with

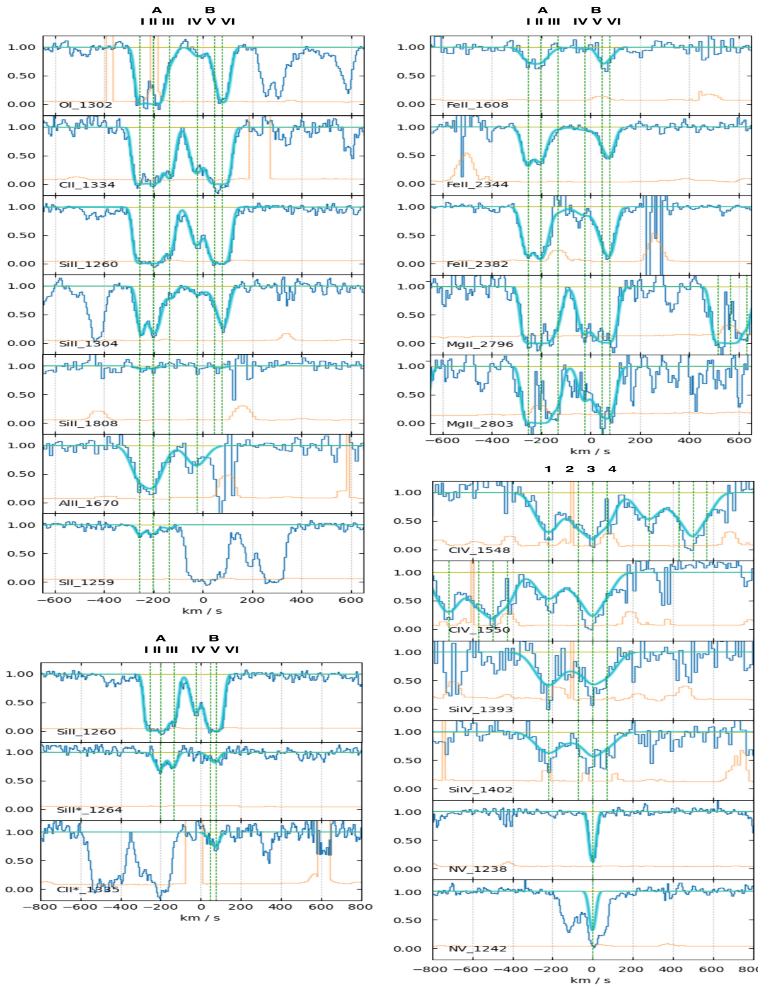

Figure 9: Observed spectra of GRB210905A through X-shooter (from [28]).

source position accuracy of $\sim$ 1.5 arcminutes; a X-ray/γ-ray Imaging Spectrometer (XGIS, 2 keV - 20 MeV), covering $\simeq$ 2 sr centered on the SXI field of view, and the InfraRED Telescope (IRT, 0.7-1.8μm) with a 10×10 arcminutes field of view, able to perform imaging and spectroscopy in real time. THESEUS will be able to find $\sim$ 2 burst yr^{-1} with spectroscopic redshift $z \simeq 8$ and $\sim$ 10 events at the same redshift determined photometrically.

Another proposed mission aiming at studying very high redshift burst is GAMOW [36, 37]. It should be equipped with a Lobster X-ray telescope (LEXT), with a $\simeq$ 1 sr field of view, a $\simeq 1'$ angular resolution and sensitive in the 0.3-10 keV range, and a Photo-z Infrared Telescope (PIRT), a 30 cm telescope operating in the 0.6-2.5 micron range, with basic photometric capabilities. GAMOW will observe in the X-ray band since the very high-redshift GRBs are expected to have a large fraction of the prompt emission redshifted in this band.

Since very few GRBs at $z > 5 - 6$ are known, it is difficult to predict the rate of event at such redshift and beyond. There are also indications that the Initial Mass Function of stars and the beaming angle of GRB jets may differ between events at high and low redshift. Nonetheless, even

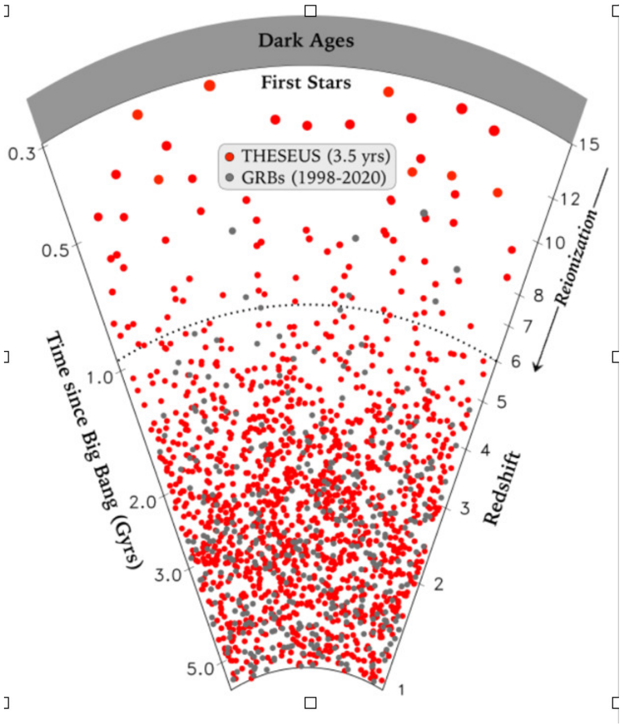

Figure 10: An example of the expected high-z GRBs that THESEUS will be able to discover and study. *Courtesy of L. Amati*.

including such uncertainties, LEXT is expected to detect $\simeq 7-12$ events at $z > 6$ yr^{-1}, an increase of about one order of magnitude with respect to Swift BAT. Moreover, GAMOW is believed to identify $\simeq 80\%$ of events at such redshifts in a ~ 1000 s timescale itself, and quickly broadcast the burst coordinates to large facilities that will begin to perform medium resolution spectroscopy. Thus, one expects an yield of ~ 8 events yr^{-1} at very high redshift and medium resolution spectroscopy.

The requirements to constrain the reionization of the Universe within a $\sim 10\%$ error is $\simeq 20$ GRBs observed with medium resolution spectroscopy at $z > 6$. We will also constrain the star formation rate at very high redshift, and if the reionization is driven by high mass stars in small galaxies which not even JCMT will detect. At the same time, GAMOW will give us precious information on the metal enrichment in the ancient past.

GAMOW was submitted to NASA MIDEX (medium-sized) mission call in 2021, but in 2022 NASA did not include it among in the selected missions. The GAMOW mission concept is at present in a revaluation phase, and a "streamlined" version of it might be submitted for the next SMEX (small-sized) call in 2025. Very likely this will be the Lobster Eye X-ray Telescope, with perhaps a GRB monitor (White et al., priv. comm.). Depending on what happens with the ESA decision on THESEUS, GAMOW may also be re-proposed for the next MIDEX round, a year or two after the SMEX call.

ESA announced in November 2023 that THESEUS is one of the three mission concepts selected for a 2.5 years Phase-A study, as a Medium science mission candidate. The next stage, which will take roughly six months, will be the Preparation of Invitation To Tender for Industrial Phase-A, selection and Kick-Off of Technical Development Activities funded through ESA/National Project Manager Committee, set-up and Kick-Off of ESA Study Team (TEST) and Science Study Team (TSST). Kick-Off of the Industrial phase A will follow, and last about one year.

7. Conclusions

The long GRB 210905A is an quite rare combination of a burst with a very high energy release, 1.27×10^{54} erg, and very high redshift, $z = 6.31$. At a few days after the trigger, it has the most luminous afterglow in the X-ray and NIR bands ever studied by Swift. However, the ratio of prompt and afterglow energetics is similar to closer and even nearby GRBs, and this burst follows the Amati, Yonetoku and Ghirlanda relations that long GRBs typically abide by. Therefore, there is not indication that this event had a peculiar progenitor, like a Population III star. We find that not only the afterglow, but the prompt emission might be explained with the Forward Shock model, usually employed to interpret the subsequent afterglow emission.

The 60 ks break in the X-ray and NIR light-curves is likely the end of mild, continuous energy injection; a later break at $\simeq$ 50 days is likely a jet break, due to an opening angle of $\theta_{jet} \simeq 0.15$ rad. This angle is larger than typical opening angles at this redshift, indicating that high redshift events do not necessarily have narrow jets. The jet break is not visible in the NIR band, likely because the afterglow is superimposed to a $H \simeq 26$ mag extended source, which we believe is the host galaxy of the GRB.

Thanks to quick X-shooter observations, we have a very detailed NIR spectrum of this host. We have a bonanza of information about metals and dust in a star forming galaxy at z=6.3, when the Universe was less than 1 billions years old. As above, the chemical abundances found do not support the hypothesis that 210905A, despite its very large energetics and its occurrence in the early Universe, was produced by a Population III star.

At present we recover only a small number of GRBs at such high redshift. Proposed missions, such as THESEUS and GAMOW, aim at detect, recognize and study several tens of GRBs at $z > 5 - 6$. This way, they will inform us about the reionization of the universe, the first galaxies, the influx of metals into the pristine medium, and perhaps the Population III stars if they end their lives as GRBs.

Acknowledgments

MDP thanks the GRAWITA collaboration for financial support to attend the Workshop. Figures 1, 2, 3, 4, 5, 6, 7, 8, and 9 are reproduced from references [16] and [28] published open access under a CC-BY 4.0 license.

References

[1] Kumar, P. & Zhang, B., 2015, PhR, 561, 1.

[2] Woosley, S., 1993, ApJ, 405, 273.

[3] Eichler, D., Livio, M., & Piran, T., 1989, Nature, 340, 126.

[4] Wang, F.-Y., Dai, Z.-G., & Liang, E.-W. 2015, NewAR, 561, 1.

[5] Gehrels, N., Chincarini, G., Giommi, P., et al., 2004, ApJ, 611, 1005.

[6] Barthelmy, S., Barbier, L., Cummings, J., et al., 2005, SSRv, 120, 143.

[7] Burrows, D., Hill, J., Nousek, J., et al., 2004, SPIE, 5165, 201.

[8] Roming, P., Hunsberger, S., Mason, K.O., et al., 2004, SPIE, 5165, 262.

[9] Aptekar, R. L., Frederiks, D. D., Golenetskii, S. V., et al., 1995, Space Sci. Rev., 71, 265

[10] Bochkarev, N., 2016, A&AT, 29, 91.

[11] Sonbas, E., Ambrosi, E., D'Ai A. et al., 2021, GCN circular 30765.

[12] Frederiks, Golenetskii, Lysenko et al. 2021, GCN circular 30780.

[13] Zerbi, F., Chincarini, G. & Ghisellini, G., 2004, SPIE, 4841, 737.

[14] Fruchter A., 1999, ApJ Letters, 512, 1.

[15] Tanvir N., Rossi A, Xu D., et al., 2021, GCN circular 30771.

[16] Rossi, A., Frederiks, D., Kann, D. A., et al., 2022, A&A, 665, 125.

[17] Sari, R., Piran, T. & Narayan, R., 1998, ApJ Letters, 497, 17.

[18] Oganesyan, G., Nava, L., & Ghirlanda, G., 2019, A&A, 628, 737.

[19] McEnery, J., 2007, 2007sngh.conf 35M

[20] Ghisellini, G., Ghirlanda, G., & Oganesyan, G., 2020, A&A, 636, 82.

[21] Zhang, B., Fan, Y.-Z., Dyks, J., et al., 2006 ApJ, 642, 354.

[22] Amati, L., 2006, MNRAS, 372, 2.

[23] Yonetoku, D, Murakami, T., Nakamura, T. et al., 2004, ApJ, 609, 935.

[24] Ghirlanda, G., Ghisellini, G., & Lazzati, D., 2004, ApJ, 616, 331.

[25] D'Avanzo, P., Salvaterra, R., Sbarufatti B., 2012, MNRAS, 425, 5.

[26] Laskar, T., Margutti, R., Alexander K., et al., 2021, GCN Circular 31127.

[27] Sari, R., Piran, T., & Halpern, J., 1999, ApJ Letters, 519, 17.

[28] Saccardi, A., Vergani, S. De Cia, A., et al., 2023, A&A, 671, 84.

[29] Zhang, W.-Q., & MacFadyen, A., 2009, ApJ, 698, 1261.

[30] Guetta, D., Spada, M., & Waxman, E., et al., 2001, ApJ, 559, 101.

PoS(MULTIF2023)070

[31] Thompson, T., 2007, RMxAC, 27, 80.

[32] Metzger, B., Giannios, D., Thompson, T. et al., 2011, MNRAS, 413, 20.

[33] Blandford, R. & Znajek R., 1977, MNRAS, 179, 4.

[34] Ghirlanda, G., Salvaterra, R., Ghisellini, G., et al., 2015, MNRAS, 448, 2514.

[35] Amati, L., O'Brien, P., Gö tz, D. et al., 2018, AdSpR, 62, 191.

[36] White, N., 2020, proc. of Yamada Conference LXXI: Gamma-ray Bursts in the Gravitational Wave Era 2019. Edited by T. Sakamoto, M. Serino and S. Sugita. Online at http://yokohamagrb2019.wikidot.com/proceedings, pp.51-53

[37] White, N., Bauer, F., Baumgartner, W., et al., 2021, AdSpR, 11821, 9.

DISCUSSION

MARIA GIOVANNA DAINOTTI: Does GRB 210905A have a plateau emission? If so, it would be interesting to show if it obeys the 3D and the 2D Dainotti relations.

MASSIMILIANO DE PASQUALE: Yes, it has plateau emission, but strangely it is very energetic. It has the plateau emission in both the X-ray and optical.

MARIA GIOVANNA DAINOTTI: Comment: Even if it is unusual, there are also cases of plateau emission at high energy, such as the cases (with?) Fermi-LAT, ApJS, 255, 1, 13, 14.